

# A phenomenological model for magnetoresistance in granular polycrystalline colossal magnetoresistive materials: The role of spin polarized tunneling at the grain boundaries

P. Raychaudhuri,<sup>a)</sup> T. K. Nath, A. K. Nigam, and R. Pinto

Tata Institute of Fundamental Research, Homi Bhabha Road, Colaba, Mumbai 400005, India

(Received 13 January 1998; accepted for publication 9 May 1998)

It has been observed that in bulk and polycrystalline thin films of colossal magnetoresistive (CMR) materials the magnetoresistance follows a different behavior compared to single crystals or single crystalline films below the ferromagnetic transition temperature  $T_c$ . In this paper we develop a phenomenological model to explain the magnetic field dependence of resistance in granular CMR materials taking into account the spin polarized tunneling at the grain boundaries. The model has been fitted to two systems, namely,  $\text{La}_{0.55}\text{Ho}_{0.15}\text{Sr}_{0.3}\text{MnO}_3$  and  $\text{La}_{1.8}\text{Y}_{0.5}\text{Ca}_{0.7}\text{Mn}_2\text{O}_7$ . From the fitted result we have separated out, in  $\text{La}_{0.55}\text{Ho}_{0.15}\text{Sr}_{0.3}\text{MnO}_3$ , the intrinsic contribution from the intergranular contribution to the magnetoresistance coming from spin polarized tunneling at the grain boundaries. It is observed that the temperature dependence of the intrinsic contribution to the magnetoresistance in  $\text{La}_{0.55}\text{Ho}_{0.15}\text{Sr}_{0.3}\text{MnO}_3$  follows the prediction of the double exchange model for all values of field. © 1998 American Institute of Physics. [S0021-8979(98)04416-8]

## I. INTRODUCTION

Hole doped  $\text{RMnO}_3$  ( $R$ =rare-earth) type perovskites have attracted considerable attention in recent times because of their unusual magneto-transport properties arising from spin charge coupling. Hole doping in these materials is achieved by partially substituting the rare-earth ion ( $R$ ) by a bivalent cation ( $M$ ) like Ca, Sr or Ba. It has been observed that the compounds of the type  $\text{R}_{1-x}\text{M}_x\text{MnO}_3$  like  $\text{La}_{0.7}\text{Sr}_{0.3}\text{MnO}_3$  or  $\text{La}_{0.7}\text{Ca}_{0.3}\text{MnO}_3$  exhibit very large magnetoresistance ( $\text{MR} \sim \Delta\rho/\rho_0 = [\rho(H) - \rho(H=0)]/\rho(H=0)$ )<sup>1-4</sup> near the ferromagnetic transition temperature. The large MR arises due to on site Hund's rule coupling between neighboring  $\text{Mn}^{3+}/\text{Mn}^{4+}$  pairs via the Zener double exchange mechanism.<sup>5</sup> According to this mechanism the hopping probability of an electron between two adjacent  $\text{Mn}^{3+}/\text{Mn}^{4+}$  is proportional to  $\cos(\theta/2)$ ,<sup>6</sup> where  $\theta$  is the angle between the two manganese spins. Thus an electron has maximum mobility when the manganese ions are parallel to each other. An applied magnetic field suppresses the spin disorder of the manganese, aligning the manganese parallel to the field. This results in increased mobility of the electrons, which in turn results in the drop of electrical resistance. Thus, below the ferromagnetic transition temperature  $T_c$  one expects the MR to be simply related to the reduction in spin fluctuation in an applied magnetic field. However one actually observes a wide variety of field dependence depending on the microstructure of the material.<sup>7-10</sup> For granular polycrystalline samples much below  $T_c$  one typically observes a sharp decrease in resistance at low fields followed by a slower almost linear decrease at higher fields. Similar behavior is also observed in polycrystalline films grown on different substrates.<sup>11</sup> On the other hand for single crystals

and single crystalline films the MR at low temperatures is very small and almost linear with the magnetic field.<sup>10,11</sup> By comparing the magnetoresistance behavior of the polycrystalline colossal magnetoresistance (CMR) material  $\text{La}_{0.7}\text{Ca}_{0.3}\text{MnO}_3$  with different grain size Mahesh *et al.*<sup>12</sup> have shown that the magnetoresistance of materials with smaller grain size is higher at temperatures below  $T_c$ , whereas the magnetoresistance at  $T_c$  does not vary significantly. These results suggest that scattering at the polycrystalline grain boundaries plays a significant role in determining the magnetoresistance in these materials in the ferromagnetic regime. Understanding the mechanism of magnetoresistance in granular polycrystalline materials is important since these materials have larger potential application due to their large magnetoresistance at low fields.

By comparing resistance versus field ( $R$ - $H$ ) data on polycrystalline bulk and single crystal of the same material, Hwang *et al.*<sup>10</sup> suggested that the low field magnetoresistance in polycrystalline materials is governed by the spin polarized transport across grain boundaries. One reason why they argued that spin polarized transport should be significant in these compounds is the high degree of spin polarization. In perovskite manganites the relatively narrow majority carrier conduction band ( $\sim 1.5$  eV) is completely separated from the minority band by a large Hund's rule as well as exchange energy ( $\sim 2.5$  eV) leading to a complete polarization of the conduction electrons.<sup>13</sup> By comparing the magnetization as a function of field ( $M$ - $H$ ) with the  $R$ - $H$  data on single crystals, Hwang *et al.* further suggested that scattering at magnetic domain boundaries in a single crystal is insignificant. Thus in this picture the low field drop in the  $R$ - $H$  curve comes due to progressive alignment of the magnetic domains associated with the grains by the movement of domain walls across the grain boundaries.

<sup>a)</sup>Electronic mail: pratap@tifrc3.tifr.res.in

Extending this idea further we develop, in this paper, a model which describes the magnetic field dependence of MR taking into account the gradual slippage of domain walls across the grain boundaries pinning centers in an applied magnetic field. The model is described in Sec. II. In Sec. III we fit the model to two CMR manganites: (i)  $\text{La}_{0.55}\text{Ho}_{0.15}\text{Sr}_{0.3}\text{MnO}_3$  which has pseudo-perovskite structure and (ii)  $\text{La}_{1.8}\text{Y}_{0.5}\text{Ca}_{0.7}\text{Mn}_2\text{O}_7$  which has a highly anisotropic layered perovskite structure. An attempt is made to separate the intrinsic contribution to the magnetoresistance in  $\text{La}_{0.55}\text{Ho}_{0.15}\text{Sr}_{0.3}\text{MnO}_3$  from the contribution coming from intergranular spin polarized transport. We have pointed out the need to separate the intrinsic contribution from the intergranular contribution in any transport measurement on bulk samples before attempting to fit the data with any theoretical model based on the double exchange mechanism.

## II. DESCRIPTION OF THE MODEL

Ferromagnets have an easy axis depending on the local crystallographic symmetry along which it is energetically favorable for the ferromagnetic spins to align. Unlike the spins inside the domains which tend to align along the easy axis, in a normal ferromagnet, the spins at the domain walls are at an angle with the easy axis which increases their anisotropy energy. Thus it is favorable for the domain wall to form at a defect site where the anisotropy energy is minimum due to the breaking of the local symmetry of the crystal. In polycrystalline materials the grain boundaries provide such pinning centers since the two adjacent grains have different anisotropy axes. Hence, in the absence of an applied magnetic field the domain wall tends to be in the grain boundary where it is pinned in a potential well, when the sample is cooled below the ferromagnetic transition temperature  $T_c$ . The free energy profile of the domain wall across grains and grain boundaries is schematically shown in Fig. 1(a). Under an applied magnetic field the magnetization reversal occurs through successive nucleation and propagation of the domain wall from the grain boundaries, with the field required to nucleate the domain boundaries higher than that required to propagate them. It is this mechanism of magnetization reversal which is known to give rise to Barkhausen jumps in many hard ferromagnets.<sup>14</sup>

In polycrystalline CMR materials the spin polarized transport across a grain boundary will give a larger resistance when the two grains have misaligned magnetization. In an applied magnetic field the domain wall experiences a force  $\mathbf{f} \propto \mathbf{M}_s \cdot \mathbf{H}$ , where  $\mathbf{M}_s$  is the spontaneous magnetization and  $\mathbf{H}$  is the applied magnetic field. When the magnetic field is large enough for the domain boundary to overcome a grain boundary pinning well [that is  $\mathbf{f} \geq [\nabla F(\mathbf{r})]_{\text{max}}$  where  $F(\mathbf{r})$  is the free energy of the domain wall (Fig. 1(b))], the domain boundary moves out of the grain boundary giving rise to a drop in the electrical resistance of the material. In the present model we further simplify things by assuming the motion of domain walls to be in one dimension. The present model starts with the following assumptions:

(i) In zero field the domain boundaries are pinned at the grain boundary pinning centers. The grain boundaries have a

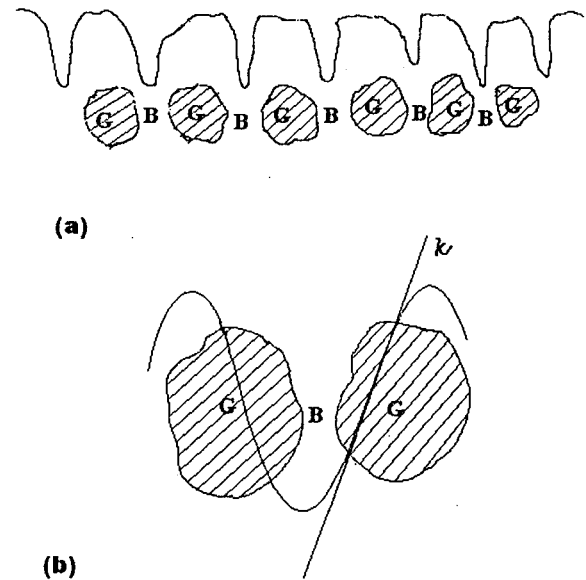


FIG. 1. (a) Free energy profile of a domain wall at grains and grain boundaries. (b) Expanded view showing the pinning strength as the maximum slope of the pinning well.

distribution of pinning strengths,  $k \sim (1/M_s)dF(x)/dx$  (defined as the minimum field needed to overcome a particular pinning barrier) given by  $f(k)$ .

(ii) When  $H \geq k$  the domain boundary slips from the grain boundary giving rise to a resistance drop  $\Delta r$ . Thus the total drop in resistance due to spin polarized tunneling at a field  $H$  is given by

$$\Delta R = N \Delta r \int_0^H f(k) dk, \quad (1)$$

where  $N$  is the number of grain boundary domain walls initially present in the sample.

(iii) Following the observations of Hwang *et al.* on single crystals we also assume that scattering at a magnetic domain boundary inside a grain is insignificant.

We further assume that the resistance has three parts: a magnetic field independent part  $R_0$  coming from nonmagnetic defects and phonon scattering, a field dependent part coming from spin polarized tunneling  $R_{\text{spt}}(H)$ , and a field dependent part coming from the reduction of spin fluctuation  $R_{\text{int}}(H)$ . Thus the total resistance  $R(H)$  can be written as

$$R(H) = R_0 + R_{\text{spt}}(H) + R_{\text{int}}(H).$$

The field dependence of the part coming from spin polarized tunneling is given by [using (1)]

$$R_{\text{spt}}(H) = R_{\text{spt}}(H=0) \left( 1 - \int_0^H f(k) dk \right), \quad (2)$$

where  $R_{\text{spt}}(H=0) = N \Delta r$ . For the field dependence of  $R_{\text{int}}(H)$  we rely on the experimental data on single crystals. It has been observed that the  $R$ - $H$  curve is predominantly linear<sup>10</sup> with a weak higher order term appearing as one approaches  $T_c$ . We assume the field dependence to be

$$R_{\text{int}}(H) = -aH - bH^3, \quad (3)$$

with the second term being significant near the ferromagnetic transition temperature  $T_c$ . Using these we get the expression for magnetoresistance as

$$\begin{aligned} \text{MR} &= [R(H) - R(H=0)]/R(H=0) \\ &= - \left( R_{\text{spt}}(H=0) \int_0^H f(k) dk + aH + bH^3 \right) / \\ &\quad [R_0 + R_{\text{spt}}(H=0)] \\ &= -A' \int_0^H f(k) dk - JH - KH^3, \end{aligned} \quad (4)$$

where

$$A' = R_{\text{spt}}(H=0)/[R_0 + R_{\text{spt}}(H=0)],$$

$$J = a/[R_0 + R_{\text{spt}}(H=0)],$$

and

$$K = b/[R_0 + R_{\text{spt}}(H=0)]$$

are the fitting parameters.

Regarding the issue of which form of  $f(k)$  would be most suitable is actually beyond the scope of the present study. However, we note that the sharp drop in the  $R$ - $H$  curve is most pronounced at low values of field. It is thus reasonable to assume that there are grain boundary pinning centers of very weak strength  $k$ . We take  $f(k)$  as a weighted average of a Gaussian and skewed Gaussian distribution:

$$f(k) = A \exp(-Bk^2) + Ck^2 \exp(-Dk^2). \quad (5)$$

The fitting parameters finally are therefore  $A$ ,  $B$ ,  $C$ ,  $D$ ,  $J$  and  $K$ , with  $A'$  absorbed in  $A$  and  $C$ .

Using this model we can now separate the spin polarized intergranular contribution from the intrinsic contribution once the fitting parameters are found using Eq. (2) and (3). It might be noted here that as a first approximation Hwang *et al.*<sup>10</sup> had earlier tried to estimate the contribution coming from spin polarized tunneling by back-extrapolating the high field linear region of the  $\text{MR}$ - $H$  curve to find the zero intercept. This method however fails at temperatures close to  $T_c$  where the high field region no longer remains linear.

### III. EXPERIMENTAL DETAILS

Magnetoresistance measurements were carried out on two CMR manganites  $\text{La}_{0.55}\text{Ho}_{0.15}\text{Sr}_{0.3}\text{MnO}_3$  which has a  $ABO_3$  type distorted perovskite structure and  $\text{La}_{1.8}\text{Y}_{0.5}\text{Ca}_{0.7}\text{Mn}_2\text{O}_7$  ( $T_c \sim 160$  K) which is an electron doped<sup>15</sup> layered perovskite with two-dimensional network of Mn-O-Mn bonds having a metal insulator transition temperature of around 135 K. The polycrystalline samples were prepared by solid state reaction starting from oxides of lanthanum, holmium, yttrium, and manganese and carbonates of strontium and calcium. Details of sample preparation are reported elsewhere.<sup>15,16</sup> We have already shown that with a small amount of holmium doping in  $\text{La}_{0.7}\text{Sr}_{0.3}\text{MnO}_3$  the  $T_c$  comes down<sup>16</sup> to suit the attainable temperature ranges of

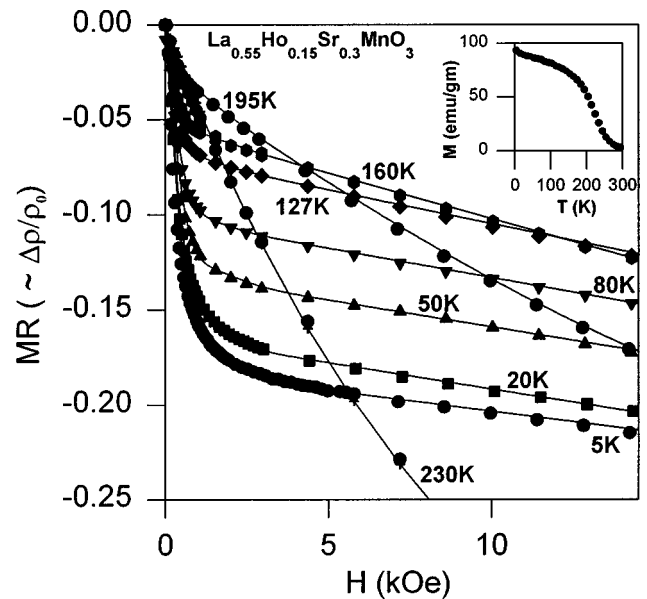


FIG. 2. The experimental  $\text{MR}$ - $H$  curves (dots) for  $\text{La}_{0.55}\text{Ho}_{0.15}\text{Sr}_{0.3}\text{MnO}_3$  and the fitted curves (lines) using Eq. (4) at various temperatures; the inset shows the magnetization as a function of temperature at 5000 Oe.

conventional low temperature cryostats. Thus for  $\text{La}_{0.55}\text{Ho}_{0.15}\text{Sr}_{0.3}\text{MnO}_3$  ( $T_c \sim 240$  K, inset Fig. 2) we measured the  $R$ - $H$  curves from 5 to 230 K. Magnetoresistance was measured using the conventional four-probe technique in magnetic fields generated by a home made superconducting magnet.

### IV. RESULTS AND DISCUSSION

Figure 2 shows the  $\text{MR}$  as a function of field ( $\text{MR}$ - $H$ ) for various temperatures as well as the fitted curves for the sample  $\text{La}_{0.55}\text{Ho}_{0.15}\text{Sr}_{0.3}\text{MnO}_3$ . To fit Eq. (4) to these curves we used the following scheme. Differentiating Eq. (4) with respect to  $H$  and putting using (5) we get

$$\begin{aligned} d(\text{MR})/dH &= A \exp(-BH^2) \\ &\quad + CH^2 \exp(-DH^2) - J - 3KH^2. \end{aligned} \quad (6)$$

The experimental curves in Fig. 2 were differentiated via the cubic spline interpolation technique and fitted to Eq. (6) to find the best fit parameters. The inset of Fig. 3 shows the differentiated curve and the best fit function at 5 K. Figure 3 shows the experimental  $\text{MR}$ - $H$  curve along with the simulated one using Eq. (4). The excellent fit of the experimental data with the simulated curve shows that this procedure is self consistent.

Figure 2 shows the fitted curves at other temperatures using Eq. (4). There is an excellent fit for all temperatures up to 230 K where the spin polarized tunnelling contribution becomes zero. The coefficient of the cubic term  $K$  is significant only at 195 K. Using the expressions for  $\text{MR}_{\text{spt}}(H)$  and  $\text{MR}_{\text{int}}(H)$  we calculate the magnetoresistance coming from intergrain spin polarized tunneling and the intrinsic contribution to the magnetoresistance at various temperatures. Figure 4 shows the temperature variation of the total magnetoresistance,  $\text{MR}_{\text{int}}(H)$  and  $\text{MR}_{\text{spt}}(H)$  at 14 kOe, respectively. We

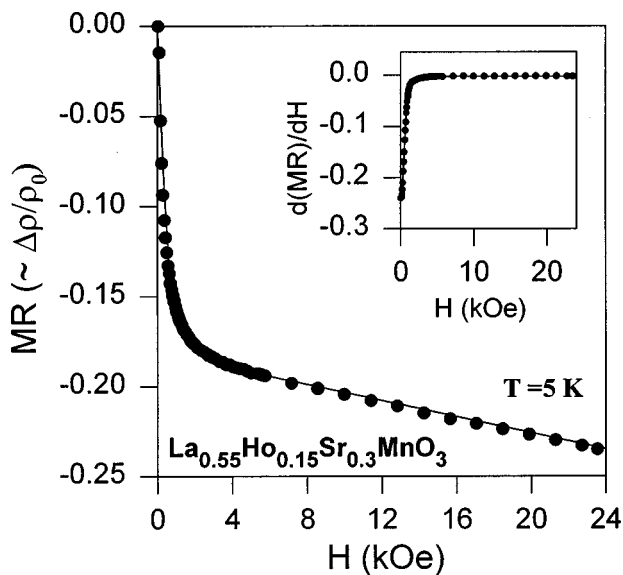


FIG. 3. The magnetoresistance vs field (MR- $H$ ) curve at 5 K: the dots (●) are the experimental points and the line (—) is the fitted curve using Eq. (4). The inset shows the derivative of the experimental curve (●) and the fitted curve (—) using the equation  $d(MR)/dH = A \exp(-BH^2) + CH^2 \exp(-DH^2) - J - 3KH^2$ , with  $A = -0.2678$ ,  $B = 2.1665$ ,  $C = -0.0125$ ,  $D = 0.4300$ , and  $J = 2.73 \times 10^{-3}$ .

observe that the total magnetoresistance is a nonmonotonic function of temperature with a slow decrease at low temperature followed by an increase as we approach  $T_c$ . The intrinsic contribution  $MR_{int}(H = 14 \text{ kOe})$ , however, follows the expected double exchange behavior with a steady increase in temperature. On the other hand  $MR_{spt}(H = 14 \text{ kOe})$  decreases steadily with temperature and totally vanishes at 230 K where the MR- $H$  curve can be fitted with a cubic polynomial only. Hwang *et al.*<sup>10</sup> had observed earlier that the tem-

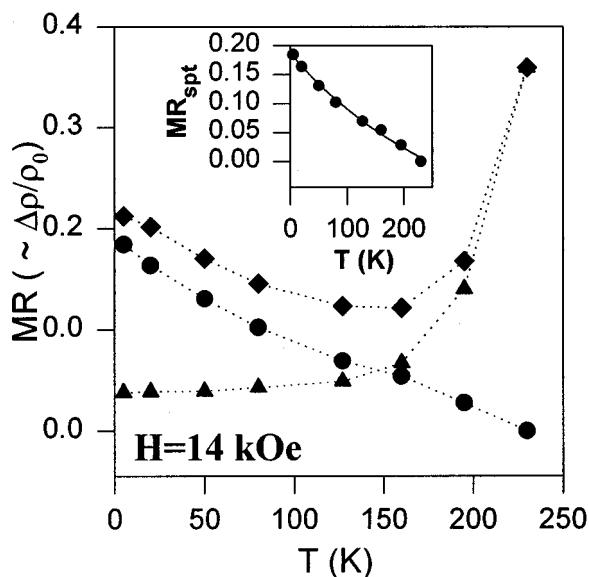


FIG. 4. Temperature dependence of various components of magnetoresistance (MR) at 14 kOe: (◆) is the total MR; (●) is the spin polarized contribution to the magnetoresistance ( $MR_{spt}$ ); (▲) is the intrinsic contribution  $MR_{int}$ . The inset shows the best fit of  $MR_{spt}$  to a function of the form  $a + b/(c + T)$ , with  $a = -0.3468$ ,  $b = 238.5 \text{ K}$ , and  $c = 446.5 \text{ K}$ .

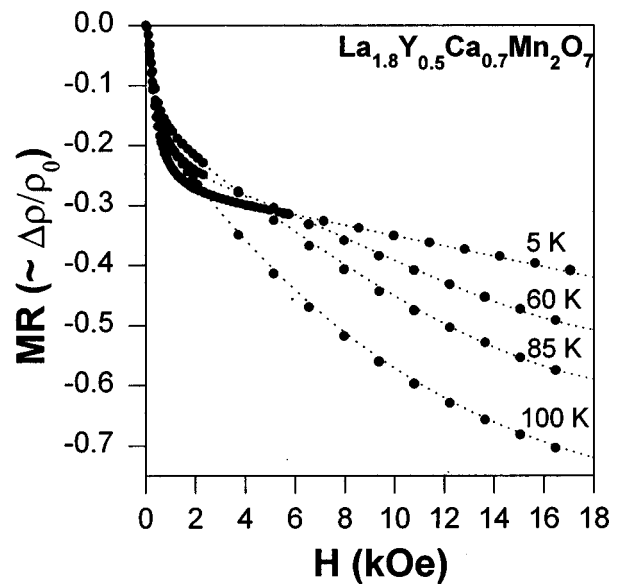


FIG. 5. The experimental MR- $H$  curves (dots) for  $La_{1.8}Y_{0.5}Ca_{0.7}Mn_2O_7$  along with the fitted curve using Eq. (4) (broken lines) at 5, 60, 85, and 100 K; The spin polarized tunneling contribution at 14 kOe [ $MR_{spt}(H = 14 \text{ kOe})$ ] at these four temperatures are 0.2634, 0.2162, 0.1583, and 0.1419, respectively.

perature dependence of  $MR_{spt}$  is described quite well by an expression of the type  $a + b/(c + T)$ , which is a characteristic of spin polarized tunneling in granular ferromagnetic systems. The inset of Fig. 4 shows the best fit of  $MR_{spt}(H = 14 \text{ kOe})$  with the expression  $a + b/(c + T)$ . The fitted curve matches well with the extracted values of  $MR_{spt}$  from the model. However our values of  $b$  and  $c$  for the best fit are much higher compared to that observed by Hwang *et al.* although the  $T_c$  of our system is much smaller. In this context we should note that the intergranular spin polarized tunneling have different temperature dependences for ferromagnetically coupled and superparamagnetically coupled grains.<sup>17</sup>

Figure 5 shows the MR- $H$  curves along with the fitted curves [with Eq. (4)] for  $La_{1.8}Y_{0.5}Ca_{0.7}Mn_2O_7$ . In this case, however, we observe the appearance of a quadratic and cubic term in  $MR_{int}(H)$  at relatively low temperatures ( $\geq 30 \text{ K}$ ). This might be related to the inherent two dimensionality of the magnetic lattice and is beyond the scope of the current paper.

### V. CONCLUSION

We have proposed a possible model for separating out the magnetoresistance arising from spin polarized transport from the intrinsic contribution in granular CMR materials. The model fits well with the experimental data on two systems, namely  $La_{0.55}Ho_{0.15}Sr_{0.3}MnO_3$  and  $La_{1.8}Y_{0.5}Ca_{0.7}Mn_2O_7$ . The intrinsic contribution follows the behavior expected from the Zener double exchange mechanism. Since the polycrystalline grain boundaries are the primary source of spin polarized tunneling, studies of the low

field behavior, for samples with controlled grain sizes will be highly interesting. Such work is currently in progress and will be published elsewhere.

## ACKNOWLEDGMENTS

The authors would like to thank S. B. Roy, C. Mitra, S. Ramakrishnan and S. Bhattacharya for their keen interest in this work. They would also like to thank S. B. Roy, P. Chad-dah, and S. Chaudhuri of Centre for Advanced Technology, Indore for their help regarding the magnetization measurement on the semiconducting quantum interference device (SQUID) magnetometer.

<sup>1</sup>R. von Helmolt, J. Wecker, B. Holzapfel, L. Schultz, and K. Samwer, *Phys. Rev. Lett.* **71**, 2331 (1993).

<sup>2</sup>R. Mahesh, R. Mahendiran, A. K. Raychaudhuri, and C. N. R. Rao, *J. Solid State Chem.* **114**, 297 (1995).

<sup>3</sup>H. L. Ju, C. Kwon, Q. Li, R. L. Greene, and T. Venkatesan, *Appl. Phys. Lett.* **65**, 2109 (1994).

<sup>4</sup>G. H. Jonker and J. H. Van Santen, *Physica (Utrecht)* **16**, 337 (1950).

<sup>5</sup>C. Zener, *Phys. Rev.* **82**, 403 (1951).

<sup>6</sup>P. W. Anderson and H. Hasegawa, *Phys. Rev.* **100**, 675 (1955).

<sup>7</sup>H. L. Ju, J. Gopalakrishnan, J. L. Peng, Q. Li, G. C. Xiong, T. Venkatesan, and R. L. Greene, *Phys. Rev. B* **51**, 6143 (1995).

<sup>8</sup>P. Schiffer, A. P. Ramirez, W. Bao, and S.-W. Cheong, *Phys. Rev. Lett.* **75**, 3336 (1995); A. P. Ramirez, *J. Phys.: Condens. Matter* **9**, 8171 (1997).

<sup>9</sup>A. Gupta, G. Q. Gong, G. Xiao, P. R. Duncombe, P. Lecoeur, P. Trouil-loud, Y. Y. Wang, V. P. Dravdi, and J. Z. Sun, *Phys. Rev. B* **54**, R15 629 (1996).

<sup>10</sup>H. Y. Hwang, S.-W. Cheong, N. P. Ong, and B. Batlogg, *Phys. Rev. Lett.* **77**, 2041 (1996).

<sup>11</sup>R. Shreekala, M. Rajeswari, K. Ghosh, A. Goyal, J. Y. Gu, C. Kwon, Z. Trajanovic, T. Boettcher, R. L. Greene, R. Ramesh, and T. Venkatesan, *Appl. Phys. Lett.* **71**, 282 (1997).

<sup>12</sup>R. Mahesh, R. Mahendiran, A. K. Raychaudhuri, and C. N. R. Rao, *Appl. Phys. Lett.* **68**, 2291 (1996).

<sup>13</sup>J.-H. Park, C. T. Chen, S.-W. Cheong, W. Bao, G. Meigs, V. Chakarian, and Y. U. Idzeral, *Phys. Rev. Lett.* **76**, 4215 (1996).

<sup>14</sup>P. J. Thompson and R. Street, *J. Magn. Magn. Mater.* **171**, 153 (1997).

<sup>15</sup>P. Raychaudhuri, C. Mitra, A. Paramekanti, R. Pinto, A. K. Nigam, and S. K. Dhar, *J. Phys.: Condens. Matter* **10**, L191 (1998).

<sup>16</sup>P. Raychaudhuri, T. K. Nath, P. Sinha, C. Mitra, A. K. Nigam, S. K. Dhar, and R. Pinto, *J. Phys.: Condens. Matter* **9**, 10 919 (1997).

<sup>17</sup>J. S. Helman and B. Abeles, *Phys. Rev. Lett.* **37**, 1429 (1976).